Dendritic but not somatic GABAergic inhibition is decreased in experimental epilepsy

R. Cossart[1], C. Dinocourt[1], J. C. Hirsch[1], A. Merchan-Perez[2], J. De Felipe[2], Y. Ben-Ari[1], M. Esclapez[1] and C. Bernard[3]

[1] *INMED, INSERM Unité 29, Avenue de Luminy, B.P. 13, 13 273 Marseille Cedex 09, France*

[2] *Instituto Cajal, 37 Ave Dr Arce, 28002 Madrid, Spain*

[3] *Present address: Division of Neuroscience, S700, Baylor College of Medicine, 1 Baylor Plaza, Houston, Texas 77030, USA*

Correspondence should be addressed to Y.B.-A. (ben-ari@inmed.univ-mrs.fr)

Impaired inhibition is thought to be important in temporal lobe epilepsy (TLE), the most common form of epilepsy in adult patients. We report that, in experimental TLE, spontaneous GABAergic inhibition was increased in the soma but reduced in the dendrites of pyramidal neurons. The former resulted from the hyperactivity of somatic projecting interneurons, whereas the latter was probably due to the degeneration of a subpopulation of dendritic projecting interneurons. A deficit in dendritic inhibition could reduce seizure threshold, whereas enhanced somatic inhibition would prevent the continuous occurrence of epileptiform activity.

GABAergic inhibition controls neuronal excitability, and compounds that increase or reduce GABAergic inhibition are used, respectively, as anti-epileptic or pro-convulsive drugs for many forms of human or experimental epilepsy[1]. For these reasons, a reduction of GABAergic inhibition is thought be important in the epilepsies. The fate of inhibition in epilepsy has been particularly studied in the hippocampus of patients with temporal lobe epilepsy, and animals with experimental TLE. Several important morpho-functional alterations have been reported in TLE: first, a loss of subpopulations of GABAergic interneurons in experimental[2–5] and human[6–8] TLE; second, an increase in $GABA_A$-receptor-mediated responses in dentate granule cells[9,10] and a decrease in responses in CA1 pyramidal cells[10,11], suggesting an area-dependent reorganization of $GABA_A$ receptor subtypes[12]; third, a deficit of GABA quantal release[11] and a modification of its control[13]. However, the consequences of these alterations in pyramidal cell inhibition are unknown. Principal cells receive continuous inhibitory input from a heterogeneous population of GABAergic neurons, which control the integrative properties of the network[14]. Based on their morphological and functional properties, two broad classes of GABAergic neurons can be distinguished: dendritic-projecting interneurons, which control the input of principal cells and the propagation of calcium currents from the dendrite to the soma, and interneurons that selectively innervate the soma of pyramidal cells, which control the generation of sodium spikes, and thus the output of principal cells[15]. To assess the fate of inhibition in TLE, it is necessary to determine the changes that occur in the two broad classes of interneurons, and the impact of these changes on the spontaneous inhibitory input to dendritic and the somatic compartments of pyramidal neurons. It is particularly important to measure the spontaneous inhibitory input, because of its strong braking effect on principal cell firing[16].

Hippocampal slices from two animal models of TLE (kainate- and pilocarpine-treated rats) were used to record the activity of all the key components of the hippocampal circuit (that is, from various interneuron subpopulations as well as from the soma and the dendrites of CA1 pyramidal cells). We report that, in TLE, tonic glutamatergic activity was increased in interneurons, leading to more frequent action potentials and consequently more frequent spontaneous inhibitory postsynaptic currents (sIPSCs) on the soma of pyramidal neurons. However, despite the hyperactivity of surviving interneurons, the net result was a reduction of tonic inhibition in the apical dendrites of pyramidal cells, probably due to the loss of a discrete but very specialized population of interneurons that projected to the distal dendrites of pyramidal neurons. Because the excitatory input was increased in the dendrites at the same time, we suggest that the decreased dendritic inhibition facilitated the generation and propagation of large dendritic excitatory postsynaptic currents (EPSCs) to the soma, whereas the increased perisomatic inhibition prevented the occurrence of persistent seizures.

Results

Selective loss of stratum oriens interneurons

GABAergic interneurons were identified by specifically labeling GAD67 (ref. 17) on sections obtained from slices adjacent to those used for patch-clamp recording. The densities of neurons labeled for either GAD67 mRNA (**Fig. 1c** and **d**) or protein (**Fig. 1a** and **b**) in strata pyramidale, radiatum and lacunosum moleculare were similar in control ($n = 6$) and epileptic ($n = 9$, pilocarpine-treated) animals. The densities, expressed as the mean number of GAD67 mRNA-containing neurons per 10,000 μm^2, were 1 ± 0.14 for control animals ($n = 30$ sections) and 1.16 ± 0.25 for epileptic animals ($n = 45$ sections) in the stratum pyramidale; in the strata radiatum and moleculare, densities were 0.54 ± 0.08 in control

animals and 0.48 ± 0.06 in epileptic animals (5 sections per animal). In contrast, there was a severe loss of neurons labeled for GAD67 protein (**Fig. 1b**) or mRNA (**Fig. 1d**) in stratum oriens and along the alveus/oriens border in epileptic animals. A decrease in the number of neurons in the stratum oriens/alveus of most pilocarpine-treated animals was evident on adjacent sections stained with cresyl violet or Neu-N, a specific neuronal marker (**Fig. 1g** and **h**). In this area, pilocarpine-treated rats lost about half of the neurons labeled for GAD67 mRNA. The density of GAD67 mRNA-containing neurons in stratum oriens was 1.51 ± 0.13 in control animals (n = 30 sections) and 0.74 ± 0.12 in epileptic animals (n = 45 sections).

Somatostatin-containing interneurons are one of the most prevalent subpopulations of GABAergic interneurons in the stratum oriens of the CA1 area[14]. Most of these neurons project massively to stratum lacunosum moleculare on the distal dendritic tree of pyramidal cells[18] (**Fig. 5b**), whereas one-third of the somatostatin-containing neurons co-express calbindin and project to the medial septum[14,19]. *In situ* hybridization for pre-prosomatostatin mRNA (**Fig. 1e** and **f**) and immunolabeling for somatostatin (**Fig. 1g** and **h**) revealed a marked decrease of labeled interneurons in stratum oriens of the CA1 area in experimental animals (n = 9) as compared to control (n = 6). There was a 46% loss of somatostatin-containing interneurons in epileptic animals (control, 0.91 ± 0.06 neurons per 10,000 μm^2, n = 30 sections; pilocarpine-treated, 0.49 ± 0.07, n = 45). Double immunohistochemical labeling for somatostatin and calbindin showed that in epileptic tissue, many of the surviving somatostatin interneurons also contained calbindin (**Fig. 1i** and **j**). These observations strongly suggest a specific loss of interneurons projecting to stratum lacunosum moleculare.

To determine whether the loss of interneurons projecting to stratum lacunosum moleculare (the so-called O-LM interneurons) was associated with a decrease in the number of symmetrical synapses in stratum lacunosum moleculare, we measured, at the ultrastructural level, the synaptic density in the neuropil of stratum lacunosum moleculare from control and pilocarpine-treated animals (**Fig. 2**). The density of symmetric synapses was similar in epileptic (1.7 ± 0.4 synapses/100 μm^2, n = 10) and control tissue (1.7 ± 0.6 synapses/100 μm^2, n = 10). However, in epileptic animals, there was a 38% shrinkage of the stratum lacunosum moleculare (see Methods; **Fig. 1a** and **b**). Taking this shrinkage into account, the estimated total number of GABAergic synapses in the stratum lacunosum moleculare of epileptic tissue was 62% of control (**Fig. 2c**).

The decrease in the number of GABAergic synapses in the stratum moleculare could correspond to a loss of GABAergic synapses per dendrite, and/or to a decrease in dendritic volume secondary to a loss of pyramidal cells (see Discussion). If the latter were the major contributing factor, a reduction in dendritic volume would also be expected in stratum radiatum. However, the dendritic processes looked similar in pilocarpine-treated and control animals, as did axonal and glial processes (**Fig. 2a**), and the width of stratum radiatum was comparable in the two groups (Methods). In addition, densities of symmetric synapses in stratum radiatum were similar in epileptic (1.8 ± 0.5 synapses/100 μm^2, n = 10) and control tissue (1.6 ± 0.5 synapses/100 μm^2, n = 10). Therefore, the decreased number of GABAergic synapses in the stratum moleculare most likely reflected a loss of GABAergic synapses per distal dendrite of CA1 pyramidal cells.

These morphological observations suggest a decrease in the inhibitory input restricted to the target synapses of O-LM interneurons in the distal apical dendrites of pyramidal neurons.

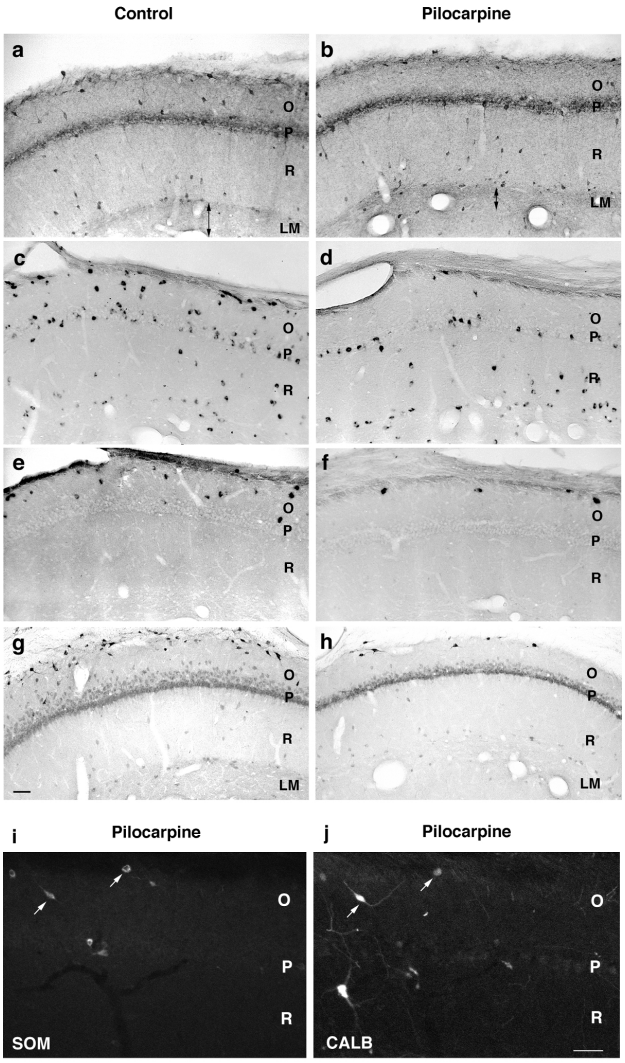

Fig. 1. GAD67-, somatostatin- and calbindin-containing neurons in the CA1 region of the hippocampal formation in control (**a**, **c**, **e**, **g**) and pilocarpine-treated (**b**, **d**, **f**, **h**, **i**, **j**) rats. (**a**, **b**) Cell bodies immunostained for GAD67 were observed throughout the hippocampal formation in controls (**a**), but only a few cell bodies in stratum oriens (O) were found in epileptic rats (**b**). In both groups, GAD67-containing terminals were most abundant in the pyramidal cell layers (P) but were also present in all the dendritic regions. Note the shrinkage in stratum lacunosum moleculare in epileptic rats (arrows). (**c**, **d**) Many cell bodies containing GAD67 mRNA were observed in CA1 of controls (**c**), whereas epileptic animals (**d**) showed fewer GAD 67 mRNA-containing neurons in the stratum oriens. (**e**, **f**) In the CA1 region, cell bodies labeled for pre-prosomatostatin mRNA were localized almost exclusively in stratum oriens in controls (**e**), but only a few of these interneurons were present in epileptic rats (**f**). (**g**, **h**) Double immunolabeling for somatostatin and Neu-N-containing neurons. The number of labeled neurons was decreased in stratum oriens of an epileptic rat (**h**) as compared to control (**g**). (**i**, **j**) Simultaneous detection of somatostatin (**i**) and calbindin (**j**) neurons showed that many remaining somatostatin-containing neurons, in the stratum oriens of a pilocarpine-treated rat, coexpressed calbindin (arrows). Scale bar, 75 μm.

Such a reduction may lead to enhanced epileptogenesis, considering the importance of the temporo–ammonic inputs of pyramidal neurons. Before directly testing this hypothesis, we examined the properties of the surviving interneurons, because they determine the inhibition received by pyramidal cell somata and dendrites.

Hyperactivity of interneurons

Interneurons were first recorded in the cell-attached configuration, which allows a non-invasive determination of the spontaneous firing frequency[20]. We recorded from 115 interneurons (n = 51 epileptic; n = 64 control) from stratum oriens, stratum pyramidale and stratum radiatum, and morphologically identified them *post hoc*. Because of the specific cell loss occurring in stratum oriens in experimental TLE, interneurons from this region and those from stratum radiatum and pyramidale are presented separately (see below).

Cell-attached recordings from interneurons of stratum radiatum and stratum pyramidale showed that 82% of the interneurons fired spontaneously in TLE (14 of 17 cells), whereas in control animals, only 41% of the interneurons discharged spontaneously (14 of 34 cells; **Fig. 3a**). Moreover, interneurons fired at a higher frequency in epileptic (9.5 ± 2.7, n = 7, 240% of control, $p < 0.05$) than in control animals (3.9 ± 0.8 Hz, n = 9, **Fig. 3a**). All classes of morphologically identified interneurons fired more frequently in experimental epilepsy, including interneurons with an axon projecting in stratum oriens (**Fig. 3c**), interneurons projecting in both stratum oriens and stratum radiatum, and perisomatic projecting interneurons (putative basket cells, n = 3 of 4 in TLE; n = 1 of 4 in control; **Fig. 4**). Therefore, most surviving interneurons in stratum radiatum and stratum pyramidale were hyperactive in experimental TLE.

The hyperactivity of stratum radiatum and stratum pyramidale interneurons likely resulted from increased glutamatergic input. Spontaneous firing of interneurons (n = 4) was suppressed by the glutamatergic antagonists CNQX (6-cyano-7-nitroquinoxaline-2,3-dione; 10 μM) and D-APV (D-2-amino-5-phosphonovaleric acid; 40 μM). In whole-cell voltage-clamp recordings, there was a 7-fold increase in the frequency of spontaneous glutamatergic currents (measured at the reversal potential of GABAergic events) in all the interneurons recorded in experimental animals (11.2 ± 2.9 Hz; n = 26, $p < 0.01$) as compared to control animals (1.6 ± 0.2 Hz; n = 26; **Figs. 3** and **4**). The increased excitatory input was uniform across the different morphological classes of interneurons, and was comparable to the increased input reported in CA1 pyramidal cells[21].

The morphological study showed a severe loss of GABAergic neurons in the stratum oriens of epileptic animals and a preferential vulnerability of O-LM cells. In control tissue, cell-attached recordings showed that O-LM interneurons fired spontaneously[22] (n = 3 of 4 cells) and received considerable glutamatergic spontaneous currents from the CA1 associational pathway (6.6 ± 2.7 Hz, n = 4, **Fig. 5**). In experimental TLE, we could not record from any O-LM cells, probably because few remained. As shown by cell-attached recordings, all surviving interneurons in stratum oriens were spontaneously active (n = 8), as compared to 62% in control (n = 8; **Fig. 5**). The interneurons in stratum oriens also received a high glutamatergic input (**Fig. 5**) and included presumed medial septum projecting interneurons (n = 3; **Fig. 5c**) and bistratified stratum oriens interneurons (n = 2).

Therefore, in experimental TLE, a subpopulation of interneurons was lost, but discharge of all populations of surviving interneurons was enhanced. We next investigated the result of these modifications by quantifying the GABAergic input to dendrites and soma of pyramidal cells.

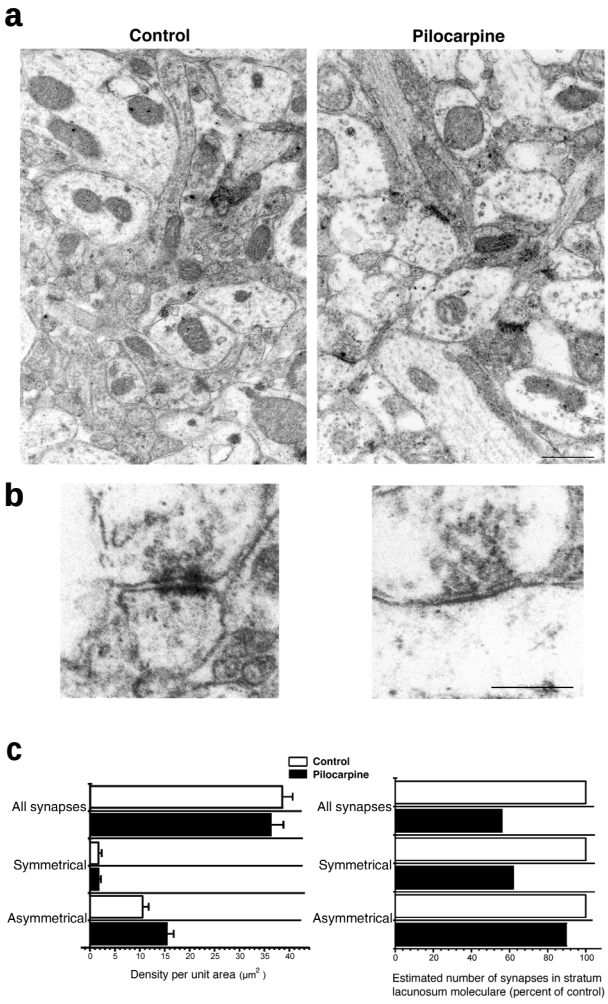

Fig. 2. Density of asymmetrical and symmetrical synapses in stratum lacunosum moleculare. (**a**) Low-power electron micrographs of the stratum lacunosum moleculare, which appears similar in control and pilocarpine-treated rats. Scale bar, 0.5 μm. (**b**) High magnification of an asymmetrical (left) and a symmetrical (right) synapse with a dendritic spine and a dendritic shaft respectively in the stratum lacunosum moleculare of a pilocarpine-treated rat. Scale bar, 0.2 μm. (**c**) Left, density of synapses in stratum lacunosum moleculare from control and epileptic animals. Right, estimated total number of each type of synapse after correction for shrinkage (38%) in epileptic tissue.

Decreased inhibition in pyramidal cell dendrites

We examined the properties of tonic inhibition in soma and dendrites of pyramidal neurons using a method previously developed[23]. Systematic *post-hoc* identification ensured that recordings were obtained from dendrites of pyramidal neurons. A dent or a hole on the biocytin-filled apical dendrite[23] indicated that the recording sites were 359 ± 58 μm and 375 ± 55 μm from the soma in experimental (n = 24) and control animals (n = 22), respectively. We recorded spontaneous IPSCs at the reversal potential of glutamatergic events (+10 mV). The frequency of IPSCs recorded in apical dendrites was significantly lower in experimental animals

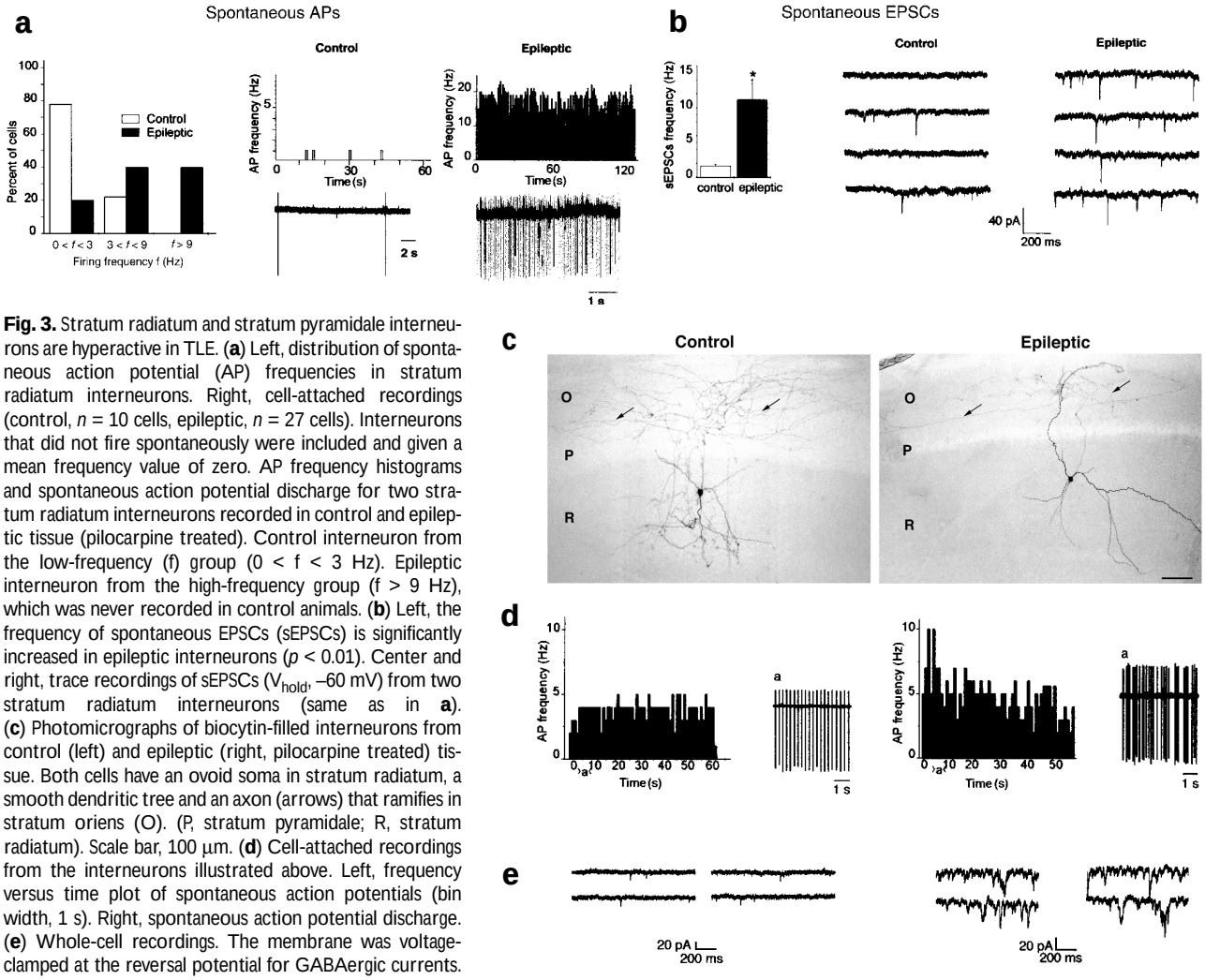

Fig. 3. Stratum radiatum and stratum pyramidale interneurons are hyperactive in TLE. (**a**) Left, distribution of spontaneous action potential (AP) frequencies in stratum radiatum interneurons. Right, cell-attached recordings (control, $n = 10$ cells, epileptic, $n = 27$ cells). Interneurons that did not fire spontaneously were included and given a mean frequency value of zero. AP frequency histograms and spontaneous action potential discharge for two stratum radiatum interneurons recorded in control and epileptic tissue (pilocarpine treated). Control interneuron from the low-frequency (f) group ($0 < f < 3$ Hz). Epileptic interneuron from the high-frequency group ($f > 9$ Hz), which was never recorded in control animals. (**b**) Left, the frequency of spontaneous EPSCs (sEPSCs) is significantly increased in epileptic interneurons ($p < 0.01$). Center and right, trace recordings of sEPSCs (V_{hold}, –60 mV) from two stratum radiatum interneurons (same as in **a**). (**c**) Photomicrographs of biocytin-filled interneurons from control (left) and epileptic (right, pilocarpine treated) tissue. Both cells have an ovoid soma in stratum radiatum, a smooth dendritic tree and an axon (arrows) that ramifies in stratum oriens (O). (P, stratum pyramidale; R, stratum radiatum). Scale bar, 100 μm. (**d**) Cell-attached recordings from the interneurons illustrated above. Left, frequency versus time plot of spontaneous action potentials (bin width, 1 s). Right, spontaneous action potential discharge. (**e**) Whole-cell recordings. The membrane was voltage-clamped at the reversal potential for GABAergic currents.

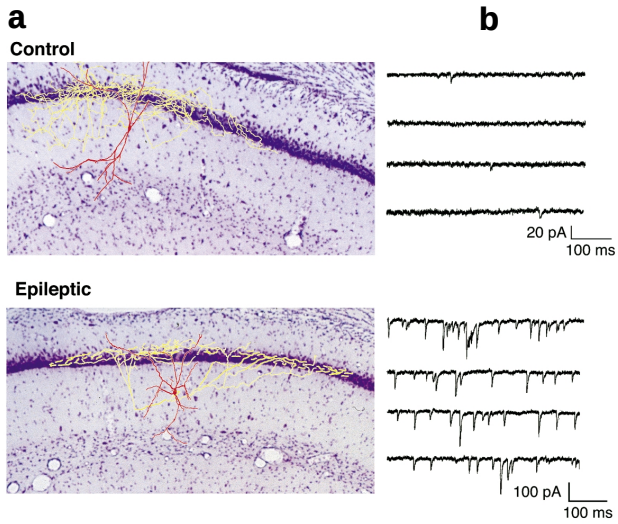

Fig. 4. Recordings from basket cells in control and epileptic rats. (**a**) Montage of presumed basket cells from a control and a kainate-treated animal. Both neurons have their soma in stratum radiatum and exhibit an extensive axonal arborization in stratum pyramidale. (**b**) Whole-cell recordings show increased spontaneous glutamatergic activity in the epileptic versus control interneuron.

(16.2 ± 3.5 Hz, $n = 16$, 73% of control, $p < 0.01$) than in controls (22.3 ± 2.7 Hz, $n = 17$; **Fig. 6**). Following application of the sodium channel blocker tetrodotoxin (TTX, 1 μM), the average frequency of miniature IPSCs (mIPSCs) was 4.9 ± 1.3 Hz ($n = 16$) in epileptic tissue, and 6.9 ± 1.8 Hz ($n = 17$) in control tissue. The ratio of miniature/spontaneous IPSC frequencies was thus comparable in experimental (29 ± 7%, $n = 16$) and control animals (28 ± 6%, $n = 17$; **Fig. 6**). To test for modification of postsynaptic $GABA_A$ receptors, we analyzed the amplitude distribution of mIPSCs. Although there was a small decrease in experimental animals (control, 12.8 ± 0.2 pA, $n = 17$; experimental, 11.8 ± 0.1 pA, $n = 16$; **Fig. 6**), in the same range as previously described in the soma[11], their kinetics did not seem modified, suggesting that postsynaptic modifications, if any, were small.

We then examined the properties of somatic inhibition. The frequency of spontaneous IPSCs recorded in the soma was not different in experimental (24.3 ± 5.1 Hz, $n = 24$) and control animals (19.8 ± 2.5 Hz, $n = 15$, $p > 0.05$; **Fig. 7**). In contrast, there was a net increase in the frequency of large-amplitude IPSCs (**Fig. 7**) and a 47% increase in the total charge underlying the IPSCs in experimental ($n = 24$) versus control animals ($n = 15$, $p < 0.01$). This increase represented the net flux of ions through $GABA_A$ receptor channels; it was not due to an increase of GABA quantal release because, as previously shown[11], the ratio of miniature/ sponta-

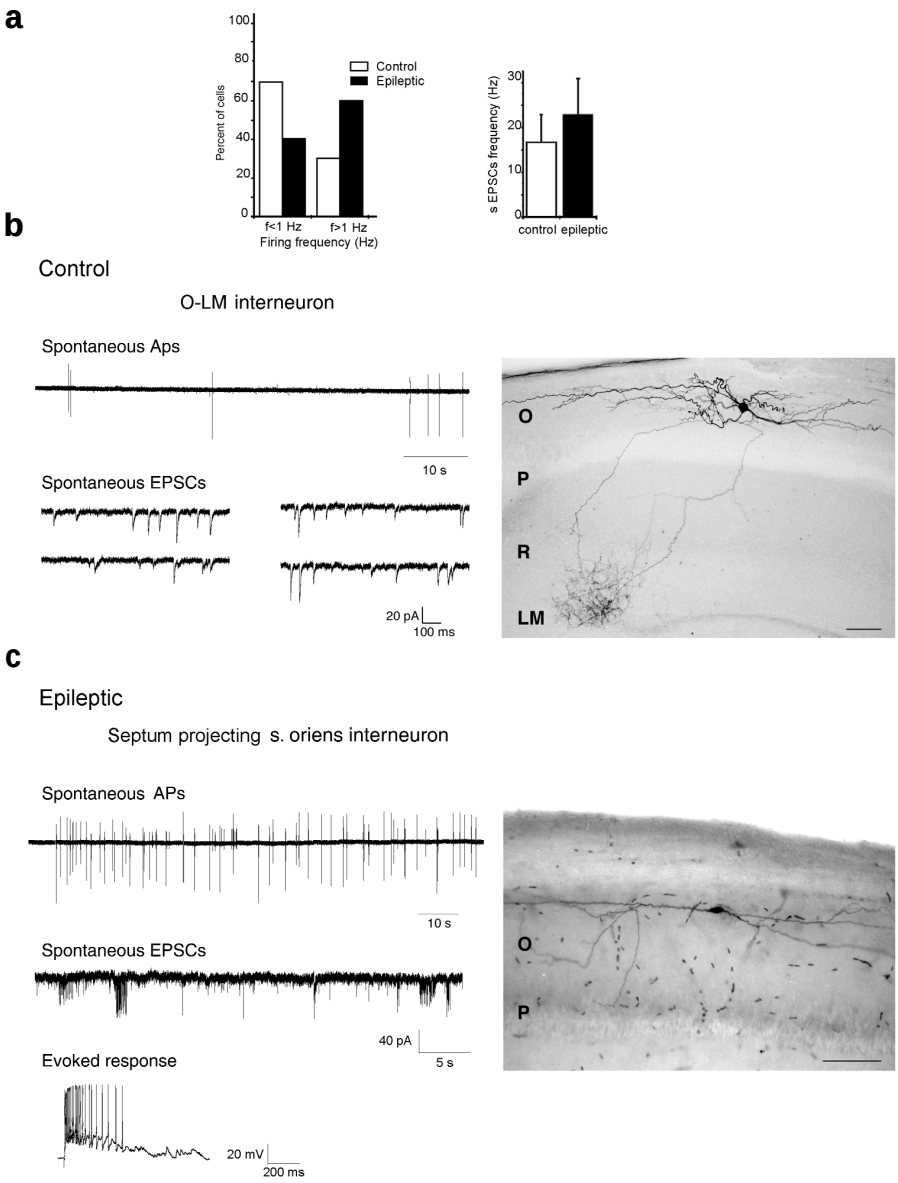

Fig. 5. Recordings from stratum oriens interneurons in control and epileptic rats. (**a**) Spontaneous action potential firing and sEPSCs frequency are increased in surviving stratum oriens interneurons. High rate of glutamatergic activity in control interneurons from stratum oriens as compared to stratum radiatum (compare with **Fig. 3b**). (**b**) Oriens-lacunosum moleculare interneuron (O-LM) in control tissue. Action potential (AP) spontaneous discharge (top, cell-attached recording) and spontaneous glutamatergic currents (bottom, V_{hold}, –60 mV). Right, the recorded interneuron with a cell body in stratum oriens, horizontally oriented dendrites and an axon that ramifies extensively in stratum lacunosum moleculare. Scale bar, 100 μm. (**c**) Presumed medial septum-projecting stratum oriens interneuron from a pilocarpine-treated animal. Action potential spontaneous discharge (top, cell-attached recording) and spontaneous glutamatergic currents (bottom, V_{hold} –60 mV). Stimulation of stratum radiatum evoked a burst of high-frequency action potentials (current clamp recording at resting membrane potential). Right, the recorded interneuron with a cell body at the stratum oriens/alveus border and an axon running along the alveus. Scale bar, 100 μm.

neous IPSC frequencies decreased from 75 ± 4% (n = 11) in control animals to 26 ± 5% (n = 10) in experimental animals (**Fig. 7**; $p < 0.001$). Therefore, the reduction of dendritic inhibition was associated with a paradoxical enhancement of the activity-dependent inhibition of the soma of pyramidal cells.

Increased excitation/inhibition ratio in dendrites

The balance between excitation and inhibition of principal cells controls the cells' spontaneous firing[16]. Because inhibitory input was decreased in the dendrites of CA1 pyramidal cells in experimental TLE, we investigated the fate of their excitatory input to evaluate the change in excitation-to-inhibition ratio.

At the ultrastructural level, the estimated number of asymmetrical synapses in stratum lacunosum moleculare was comparable in epileptic and control animals (**Fig. 2**). Still, the shrinkage of the lacunosum moleculare probably modified the distribution of asymmetrical synapses on distal dendrites, as suggested by the increased density of asymmetrical synapses in pilocarpine-treated (15.4 ± 1.3 synapses/100 μm^2, n = 10) versus control animals (10.6 ± 1.2 synapses/100 μm^2, n = 10). The ratio of asymmetrical to symmetrical synapses in lacunosum moleculare was thus increased about 46% in experimental animals.

At the physiological level, spontaneous EPSCs were recorded at –60 mV and IPSCs at +10 mV to determine their ratio for each recorded dendrite. This ratio was increased in epileptic (18 ± 4%, n = 13) as compared to control animals (9 ± 2%, n = 13, $p < 0.05$). Thus, in experimental TLE, the balance between excitation and inhibition is tipped toward excitation.

Epileptic activity in pyramidal cell dendrites

In control slices, blocking activity of stratum oriens interneurons increases the amplitude of stratum radiatum field EPSPs[24], which suggests that O-LM interneurons control the excitability of pyramidal neurons' dendrites. In epileptic tissue, which lacks a subpopulation of stratum oriens interneurons, stimulation of the stratum radiatum evoked graded epileptiform discharges in the apical dendrites of CA1 pyramidal cells, in contrast to the single action potential evoked by comparable stimulation in control tissue[21]. Furthermore, in the dendrites of epileptic rats, as previously reported for the soma[25], the NMDA receptor antagonist D-APV decreased the number of action potentials overriding the epileptiform burst discharge evoked by suprathreshold stimulation (n = 4, **Fig. 8a**), suggesting that NMDA receptors actively participated in the generation of these evoked epileptiform discharges.

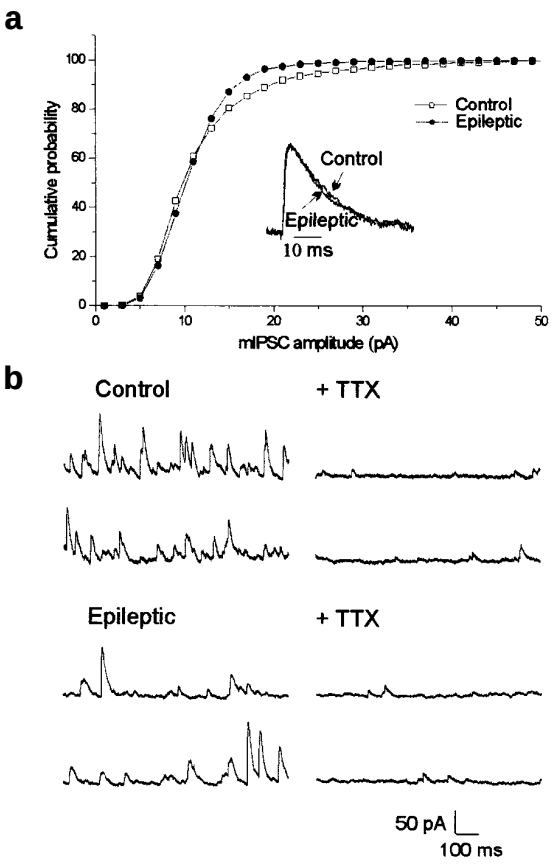

Fig. 6. Recordings from the apical dendrites of CA1 pyramidal cells. (**a**) The cumulative probability plot of the amplitudes of miniature events was shifted to the left, indicating a decreased frequency of amplitudes larger than 15 pA in epileptic animals. The kinetics of miniature events (normalized averages) did not seem modified (inset). Rise time, 0.99 ms (control) and 0.98 ms (epileptic); decay time, 9 ms (control) and 10 ms (epileptic). (**b**) Whole-cell recordings of spontaneous (control) and miniature (TTX, 1 μM) inhibitory postsynaptic currents obtained at the reversal potential of glutamatergic events in a control and a kainate-treated animal. Continuous 4-s recordings are shown. The frequency of spontaneous events is lower in the epileptic tissue.

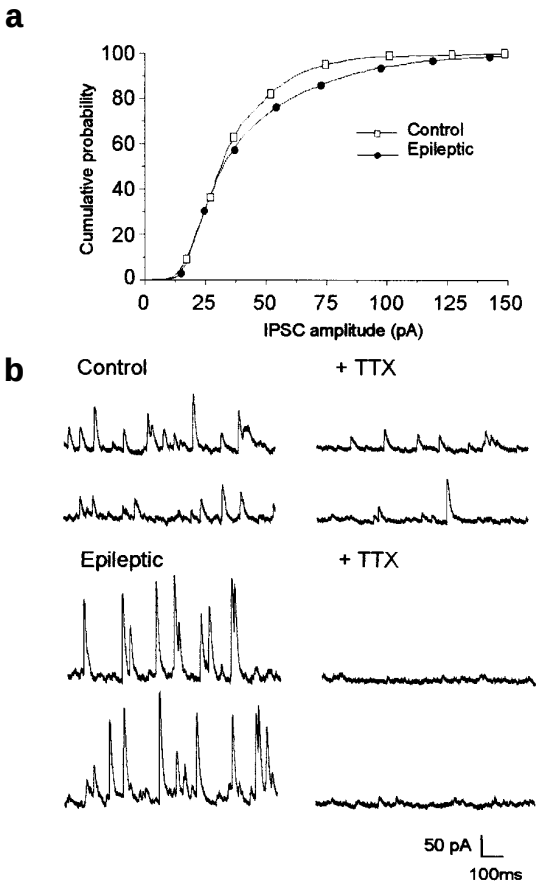

Fig. 7. Somatic recordings from CA1 pyramidal cells. (**a**) The cumulative probability plot of the amplitudes of spontaneous IPSCs was shifted to the right, indicating an increased frequency of large-amplitude events in experimental animals (n = 6 cells) as compared to controls (n = 6 cells). (**b**) Whole-cell recordings of spontaneous (control) and miniature (TTX, 1 μM) inhibitory postsynaptic currents obtained at the reversal potential of glutamatergic events. The frequency of spontaneous events was similar in control and epileptic neurons, but the number of large-amplitude events seemed increased in the epileptic neuron. The frequency of miniature events is considerably decreased in the epileptic neuron.

One function of the inhibition provided by O-LM cells is to control the temporo–ammonic pathway, which projects to stratum lacunosum moleculare[26]. The loss of O-LM cells in experimental TLE should favor the propagation of temporo–ammonic pathway EPSPs and action potential firing. To address this issue, we compared the responses evoked by stimulating the direct temporo–ammonic pathway to the CA1 region in control and epileptic tissue (**Fig. 8b** and **c**). The initial slope of the EPSP was measured as a function of the stimulus intensity (input/output curves); in the range of stimulation used, the curves were linear (**Fig. 8c**). The mean slope of the curve in epileptic tissue increased by 800% relative to control (**Fig. 8c**), demonstrating that sizeable EPSPs were obtained with much lower stimulus intensities in experimental animals. The stimulus intensity needed to generate an action potential was lower in TLE than in control (**Fig. 8c**). Furthermore, activation of the perforant path could generate a burst of action potentials in epileptic animals (n = 5, **Fig. 8c**) whereas the same stimulus intensity applied in the same conditions in control animals triggered, at most, one action potential (n = 4, **Fig. 8c**). Thus the excitatory pathway from entorhinal cortex to CA1 was facilitated in TLE.

Discussion

We report a domain-specific modification of the GABAergic inhibition of pyramidal cells in chronic epilepsy: a reduction in the dendrites and an increase in the soma. We propose that this dual alteration is due to selective loss of O-LM cells (reducing dendritic inhibition) and to hyperactivity of the surviving interneurons (increasing somatic inhibition). We therefore suggest that chronic epilepsy permanently modifies the input/output relationship in principal cells, enhancing control over hippocampal output via increased somatic inhibition, but also causing permissiveness to excitatory inputs (in particular, those from the perforant path) via the decrease of dendritic inhibition.

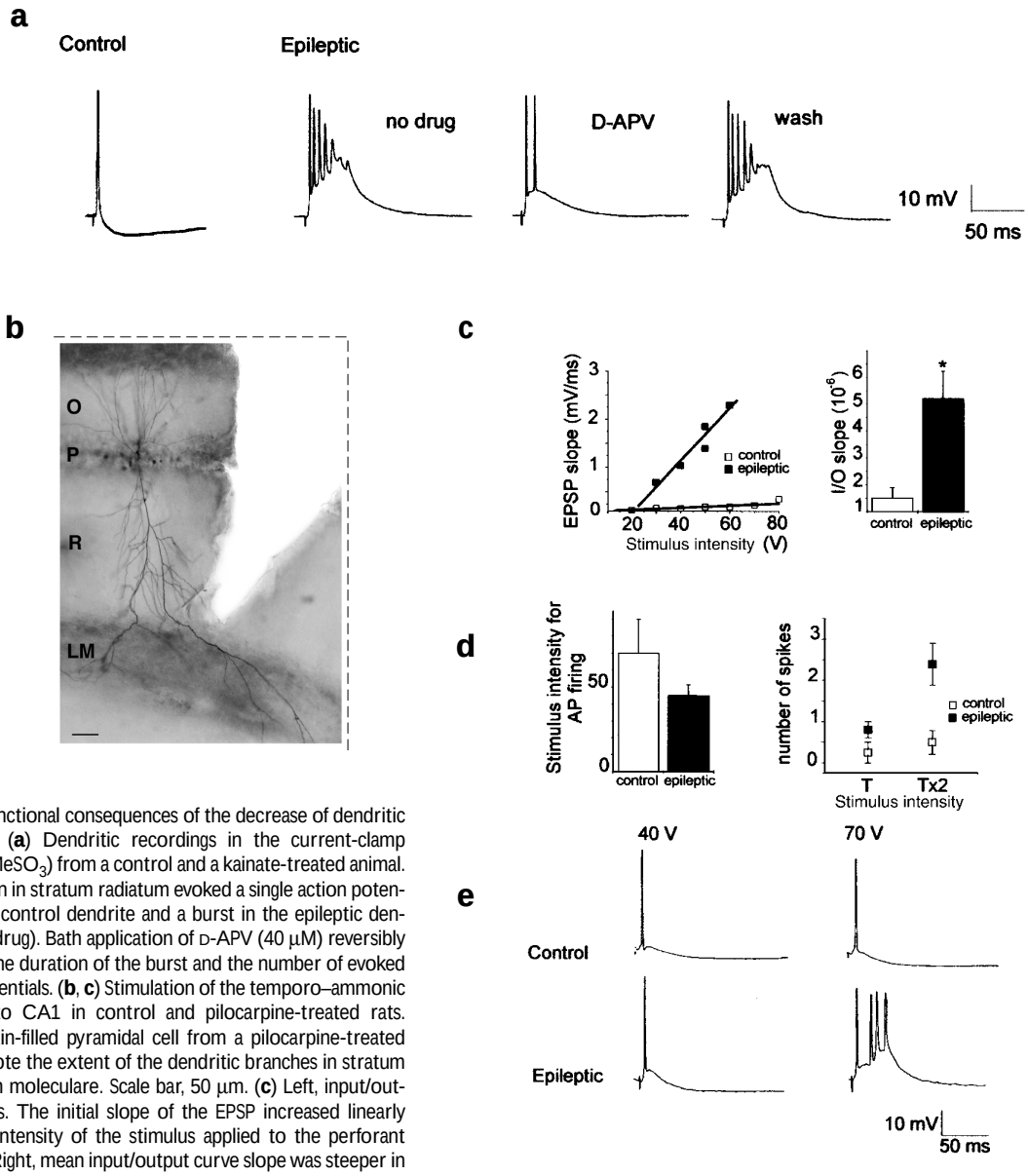

Fig. 8. Functional consequences of the decrease of dendritic inhibition. (**a**) Dendritic recordings in the current-clamp mode ($KMeSO_3$) from a control and a kainate-treated animal. Stimulation in stratum radiatum evoked a single action potential in the control dendrite and a burst in the epileptic dendrite (no drug). Bath application of D-APV (40 μM) reversibly reduced the duration of the burst and the number of evoked action potentials. (**b**, **c**) Stimulation of the temporo–ammonic pathway to CA1 in control and pilocarpine-treated rats. (**b**) Biocytin-filled pyramidal cell from a pilocarpine-treated animal. Note the extent of the dendritic branches in stratum lacunosum moleculare. Scale bar, 50 μm. (**c**) Left, input/output curves. The initial slope of the EPSP increased linearly with the intensity of the stimulus applied to the perforant pathway. Right, mean input/output curve slope was steeper in cells from epileptic ($n = 4$) than from control ($n = 4$) animals. (**d**) Left, intensity of stimulation applied to the perforant path necessary to reach AP threshold (T) in cells from control (T = 70 V, $n = 4$) and epileptic slices (T = 40 V, $n = 5$). Right, the mean number of action potentials evoked at the mean threshold and twice the mean threshold ($T \times 2$) was higher in epileptic than in control cells. Current-clamp recordings of the soma of CA1 pyramidal cells ($KMeSO_3$). (**e**) In a control cell, increasing the stimulation of the perforant path from threshold for action potential generation (40 V) to 70 V evoked at most a single spike. In a cell from a pilocarpine-treated animal, the same stimuli evoked one (40 V) or a burst (70 V) of action potentials.

Loss of O-LM interneurons

GABAergic and somatostatin-containing interneurons in the hilus of the dentate gyrus are lost in experimental and human TLE[2,4,6–8,27]. Confirming preliminary observations[4], we now report GAD-containing neuron loss in the stratum oriens of the CA1 region of pilocarpine-treated rats with chronic limbic seizures. This loss was due to cell death, as both GAD mRNA and protein were reduced, along with the number of neurons labeled with cresyl violet or Neu-N. Among the GABAergic neurons that degenerated in stratum oriens, somatostatin-containing neurons were particularly vulnerable (46% of neuronal loss). In control tissue, somatostatin-containing interneurons in stratum oriens comprise O-LM, bistratified cells[28,29] as well as medial septum-projecting interneurons that also express calbindin[19]. In epileptic tissue, most somatostatin-containing neurons that co-express calbindin survived, and the only cell types we could record from were bistratified and medial septum-projecting interneurons. Together, these observations strongly suggest that the somatostatin-containing neurons that degenerated in stratum oriens were O-LM interneurons. Because O-LM neurons form symmetric synapses primarily on the distal dendrites of pyramidal cells[18] at the site of perforant path afferences, a loss of GABAergic synapses was expected in stratum lacunosum moleculare.

At the ultrastructural level, the estimated loss of one-third of symmetric synapses in stratum lacunosum moleculare could decrease either the number of GABAergic synapses per dendrite, and/or dendritic volume (resulting from neuronal loss or reduced dendrite number and/or length). Because most interneurons that degenerate do not send dendrites to stratum lacunosum moleculare (as do O-LM cells), a decrease in dendritic volume would principally originate from the death of pyramidal cells or from a decrease in their dendrite number and/or length. Several findings are not consistent with the hypothesis of a major dendritic loss. First, in pilocarpine-treated animals, the death of CA1 pyramidal cells is marginal (much less than 10%)[30]. Second, dendritic and glial processes looked similar in control and epileptic tissue. Third, the depth of stratum radiatum and the number of GABAergic synapses in this region were not modified in pilocarpine-treated animals. Fourth, in pilocarpine (data not shown) as well as in kainate models of TLE, the length and number of dendritic branches in CA1 pyramidal cells increased, not decreased, because of dendritic sprouting[31]. Thus, loss of symmetric synapses in stratum lacunosum moleculare most likely reflects fewer GABAergic synapses in the distal part of the dendritic tree of pyramidal cells due to the loss of O-LM cells.

Network plasticity

The reactive plasticity of glutamatergic pathways is a major characteristic of epileptic tissue. In many animal models of TLE and in human patients, axonal sprouting is associated with the formation of new synapses. This sprouting is best documented for the mossy fiber pathway (for review, see ref. 32). Similar observations have been made for the axons of CA1 pyramidal neurons in kainate- or pilocarpine-treated rats[21,33]. Here we show that the frequency of spontaneous glutamatergic currents is increased in interneurons from animals with TLE. In the same models of TLE, a comparable increase in spontaneous glutamatergic currents in pyramidal cells is associated with sprouting of the CA1 associational pathway in strata oriens, pyramidale and radiatum, and probably leads to the formation of new functional synapses[21]. Thus, it is likely that the increased connectivity resulting from the axonal sprouting of principal cells is not restricted to other pyramidal cells, but also involves new connections with interneurons. The increased glutamatergic input to interneurons in experimental TLE directly contributes to their hyperactivity, although other factors, such as a modification of their membrane properties, cannot be ruled out[34]. However, a general increased level of interneuron excitation is consistent with the observation that stimulation of excitatory afferents triggers epileptiform discharges in surviving interneurons[35,36].

Dual alterations of spontaneous inhibition in TLE

Therefore, in TLE, glutamatergic axons seem to innervate their various targets, including interneurons, more extensively. This increased glutamatergic input leads to an enhanced GABAergic input to principal cell somata, suggesting that seizures are associated with a paradoxical enhancement of tonic inhibition[37–39]. Our data suggest that inhibition changes in TLE are domain-specific, that is, they are compartmentalized along the somato–dendritic axis of pyramidal cells.

This conclusion requires that somatic and dendritic recordings reflect input from two distinct somatic- and dendritic-projecting inhibitory pathways. Currents recorded in the soma are theoretically a mixture of synaptic events generated in the soma and dendrites, even if imperfect space clamp and the complex electrotonic properties of large adult neurons prevent proper access to dendrites when recording from the soma[23]. When simultaneous somatic and dendritic recordings of the same pyramidal neuron are made, small amplitude currents measured in the dendrites more than 150 μm away from the soma are not detected in the soma[40]. Likewise, dendritic IPSPs are not significantly altered when the soma is voltage-clamped (J. Magee, personal communication). Furthermore, in our conditions, contamination of dendritic recordings by events generated in the soma is limited to large-amplitude events[23]. Therefore, IPSCs recorded in the dendrites and the soma mostly represent locally generated events. These considerations support our hypothesis that in pyramidal cells, the dendritic- and somatic-projecting inhibitory pathways can be characterized by dendritic and somatic recordings, respectively. Thus, there are two different, pathway-specific alterations of the GABAergic input to CA1 pyramidal cells in experimental TLE.

In the soma of CA1 pyramidal cells, action-potential dependent IPSCs occurred at a higher frequency than in control, with a significant increase in charge transfer through the membrane. This increased GABAergic input is likely due to the hyperactivity of perisomatic projecting interneurons, a population of cells relatively resistant in TLE[32] (also see present results). Because spontaneous GABAergic input tightly controls the firing of principal cells[16], the increased inhibitory input we report would effectively counterbalance the increased excitatory input to CA1 pyramidal cells that occurs in experimental TLE.

In apical dendrites, all the modifications decreased GABAergic inhibition. First, miniature GABAergic activity decreased. (Whether this is a direct consequence of GABAergic synapse loss or a deficit of GABA quantal release remains to be investigated.) Second, frequency of action-potential-dependent IPSCs significantly decreased (**Fig. 6**), despite the hyperactivity of the surviving dendritic-projecting interneurons (**Figs. 4** and **5**). Our morphological and physiological data strongly suggest that this decrease mainly resulted from the loss of O-LM cells, a population of neurons particularly active in control tissue. The inhibition deficit in the distal dendritic tree, combined with the increased excitatory input, greatly modified the ratio of glutamatergic to GABAergic input during steady state. Because the amplitude of glutamatergic events increases with the distance to the soma[40], distally, the balance between excitation and inhibition will be further tipped toward excitation, creating permissive conditions for large glutamatergic events to travel toward the soma. Reducing the tonic inhibitory input on distal dendrites could have direct pro-epileptic consequences, by facilitating the excitatory input from the entorhinal cortex as shown here. Such a reduction could also facilitate sodium and calcium currents[41], the NMDA-receptor-mediated component of EPSCs[41,42], and the backpropagation of action potentials in dendrites[43]. The finding that NMDA receptors directly participated in epileptiform discharges in the dendrites of epileptic animals supports this hypothesis. Perhaps the most important consequence of the O-LM cell loss is the facilitation of the direct temporo–ammonic pathway. In control CA1, stimulation of excitatory inputs generates epileptiform discharges when the inhibitory input from stratum oriens interneurons is blocked[24]. Thus, in TLE, the activation of the temporo–ammonic pathway can generate epileptiform bursts in pyramidal cells (although increased boosting of excitatory events through activation of voltage-gated cation channels cannot be ruled out). It now needs to be addressed whether the selective decrease of tonic inhibition in the dendrites and the facilitation of the direct temporo–ammonic pathway is important in the generation and propagation of spontaneous seizures.

In conclusion, the extensive morphological alterations that occur in TLE—cell death and synaptic reorganization—lead to a permanent imbalance between the two components of inhibition: an increase in somatic inhibition and a decrease in distal dendritic inhibition. The first component may be a key factor in keeping the system under control most of the time, whereas the second, in association with the increased excitatory input, would tend to reduce seizure threshold. The development of therapeutic strategies to treat drug-resistant forms of TLE should take into account the duality of the alterations in GABAergic input.

METHODS

Animals. Adult male Wistar rats (180–200 g) were treated with pilocarpine or kainate according to established procedures[2,44]. Briefly, pilocarpine (325–340 mg/kg) was injected intraperitoneally 30 min after a low dose of cholinergic antagonist methyl scopolamine nitrate (1 mg/kg, i.p.) to minimize peripheral cholinergic effects. Kainate (0.5 μg in 0.5 μl phosphate buffer, pH 7.4) was infused over 30 min into the left lateral ventricle under chloral hydrate (350 mg/kg) anesthesia. After recovery from the acute seizures induced by the drugs, rats were observed periodically in the vivarium for spontaneous seizures. Kainate- (n = 28) and pilocarpine-treated rats (n = 27) that had spontaneous limbic seizures were selected (1–24 months after drug injection). Age-matched rats (n = 30) were used for control experiments. All animal use protocols conformed to the NIH guidelines and the French Public Health Service policy on the use of laboratory animals.

Electrophysiology. Animals were intracardially perfused, under chloral hydrate (350 mg/kg) anesthesia, with modified artificial cerebrospinal fluid (ACSF), and 400-μm-thick slices were prepared with a Leica VT 1000E (Nussloch, Germany) tissue slicer as described[25]. ACSF contained 124 mM NaCl, 3 mM KCl, 1.25 mM KH_2PO_4, 26 mM $NaHCO_3$, 1.3 mM $MgSO_4$•$7H_2O$, 2 mM $CaCl_2$, 10 mM D-glucose, and was continuously aerated with 95% O_2 and 5% CO_2. The temperature in the submerged recording chamber was maintained at 30–32°C. Spontaneous postsynaptic currents were recorded from somata or dendrites of CA1 pyramidal neurons (using the blind technique) with tight-seal, whole-cell patch-clamp pipettes. Interneurons were recorded in the cell-attached configuration using infrared imaging. Slices were transferred to a chamber on the stage of an Axioscope Karl Zeiss microscope (Jiena, Germany) or a Leica DM LFS microscope. Interneurons were identified using IR-DIC (infrared-differential interference contrast) microscopy through a 40× water-immersion objective. Microelectrodes had a resistance of 4–12 MΩ, and we used internal solutions of the following compositions: for voltage-clamp recordings, 135 mM Cs-gluconate, 10 mM $MgCl_2$, 0.1 mM $CaCl_2$, 1 mM EGTA, 2 mM Na_2 adenosine triphosphate, 10 mM HEPES, 0.5% biocytin, pH 7.25; for current clamp recordings, Cs-gluconate was replaced by K-methanesulfonate. The osmolarity of the internal solutions was between 265 and 275 mOsm. All recorded pyramidal cells and interneurons were morphologically identified *post hoc*.

We measured spontaneous inhibitory currents at the reversal potential for glutamatergic events (around +10 mV), as described[36]. Bicuculline was applied at the end of the experiments to verify that the currents were indeed GABAergic[36]. Spontaneous glutamatergic currents were measured at the reversal potential for GABAergic events and were blocked by CNQX and D-APV[21]. The temporo–ammonic pathway to the CA1 region was stimulated in control and epileptic tissues as described[26]. The perforant pathway was isolated with a cut that severed the entorhinal cortex input to the dentate gyrus, and a second cut was made in the CA1 area from the stratum oriens to the stratum radiatum/lacunosum moleculare border (**Fig. 8b**) to prevent the spread of the stimulating current to the Schaffer collateral pathway. The stimulating electrodes were positioned in stratum lacunosum moleculare on the side of the cut opposite the recorded cell. Bicuculline, kainate, pilocarpine, methyl scopolamine nitrate and biocytin were obtained from Sigma (St. Louis, Missouri) and TTX from Latoxan (Rosans, France). D-APV and CNQX were donated from Novartis (Basel, Switzerland). Signals were fed to an Axopatch 200A,B amplifier (Axon Instruments, Foster City, California) or a EPC9 (HEKA, Heidelberg, Germany). All data were digitized (10 kHz) with a Labmaster (Axon Instruments) interface card to a personal computer and analyzed with Acquis1 program (G. Sadoc, 1994, Biologic, Grenoble, France). Data are given as mean ± s.e.m and compared with Student's t-test. Because there was no statistical difference between the results obtained from pilocarpine- or kainate-treated rats, data were pooled.

Light microscopy. All recorded slices were processed for biocytin-filled neuron detection. In addition, some hippocampal slices from nine pilocarpine-treated and six control animals were collected immediately after slice preparation for non-radioactive *in situ* hybridization histochemistry and immunohistochemistry. Slices were fixed overnight at 4°C in 4% paraformaldehyde in 0.1 M phosphate buffer (PB, pH 7.4), rinsed in PB, cryoprotected in sucrose and quickly frozen on dry ice. Slices to be processed for histochemistry were resectioned (40 μm) on a cryostat. Sections were rinsed in 0.01 M phosphate-buffered saline, pH 7.4 (1× PBS), collected sequentially in tubes containing an ethylene glycol-based cryoprotective solution and stored at –20°C until processing. From each animal, adjacent sections were processed for non-radioactive *in situ* hybridization with GAD67 and pre-prosomatostatin cRNA probes and for immunohistochemistry with antibodies that are specific for somatostatin, calbindin and the GAD67 isoform.

GAD67 and pre-prosomatostatin mRNA were detected with digoxigenin-labeled riboprobes produced by *in vitro* transcription of the corresponding cDNAs. The GAD67 cDNA (2.7kb) was a subclone of the GAD67 clone that was isolated from a λgt-11 rat whole-brain library using a feline GAD67 cDNA and subcloned into a bluescript vector[45]. The localization of GAD67 mRNA was used here because previous *in situ* hybridization studies demonstrated that GAD67 mRNA is present in all groups of GAD- and GABA-containing neurons in the hippocampal formation[17]. The rat pre-prosomatostatin cDNA (0.4 kb) was isolated from a rat medullary thyroid carcinoma library and subcloned into a Sp65 vector[46]. This cDNA contained the entire coding region of the rat pre-prosomatostatin, the common precursor of somatostatin-14 and somatostatin-28, the biologically active peptides. Transcription was done with the nonradioactive RNA labeling kit (Boehringer Mannheim, Indianapolis, Indiana) as described[47]. Transcripts labeled with digoxigenin-11-UTP were fragmented by limited alkaline hydrolysis to obtain probes of approximately 160 nucleotides in length.

Free-floating sections were processed for GAD67 and pre-prosomatostatin non radioactive *in situ* hybridization as described[47]. Briefly, after standard pretreatments to enhance penetration of the reagents, sections were incubated for 1 h at room temperature in the prehybridization solution, and for 16 h at 50°C in hybridization solution containing 0.2 ng/μl digoxigenin-labeled RNA probe. Sections were treated with ribonuclease A (50 μg/ml) and low to high stringency washes were done with decreasing concentrations of saline sodium citrate (SSC), ending with an incubation in 0.1× SSC, 10 mM sodium thiosulfate for 30 min at 55°C (1× SSC, 150 mM NaCl, 60 mM Na citrate, pH 7.0). Sections were then processed for immunodetection of the digoxigenin label with a nucleic acid detection kit (Boehringer Mannheim; for details, see ref. 47). Sections from control and pilocarpine-treated animals were processed in parallel under identical experimental conditions (including the incubation time) in the chromogen solution (2 h for GAD and pre-prosomatostatin mRNAs in each of the two animal groups). Sections were mounted on gelatin-coated slides, dried and coverslipped in an aqueous mounting medium (Crystal/Mount, Biomeda, Foster City, California).

Preparation and characterization of the polyclonal antiserum K2, used to localize GAD67, have been described[48]. We used a polyclonal rabbit antiserum (IHC 8001, Peninsula Laboratories, Belmont, California) that recognizes both somatostatin-14 and somatostatin-28 peptides. We used a monoclonal antibody that recognizes the neuron-specific protein Neu-N (MAB 377, Chemicon, Temecula, California) to visualize all hippocampal neurons, and a mouse monoclonal antibody D-28K (McAB 300, Swant, Bellinzona, Switzerland) to localize calbindin.

Sections from control and pilocarpine-treated animals were processed in parallel for GAD67 or somatostatin immunohistochemistry by unlabeled antiserum and standard avidin-biotin-peroxidase immunolabeling methods (Vectastain Elite Rabbit IgG Kit, Vector, Burlingame

California) as described[47] with a few modifications for tissue fixed by immersion. Sections were washed in 0.02 M potassium phosphate-buffered saline (KPBS, pH 7.4), used throughout these experiments. To block endogenous peroxidase, sections were incubated in 1% hydrogen peroxide for 30 min. Sections were then incubated for 1 h at RT in 3% normal goat serum with (GAD67 and somatostatin) or without (GAD67) 0.3% Triton X-100 . Sections processed for GAD67 were then incubated for 20 h at room temperature (RT) in K2 antiserum, diluted 1:4000 in KPBS containing 1% normal goat serum. We incubated sections processed for somatostatin for 48 hours at 4°C in the primary antiserum diluted 1:4000 in KPBS containing 1% normal goat serum and 0.3% Triton X-100. Following incubations, sections were rinsed for 30 min in KPBS, incubated for 1 h at RT in biotinylated goat anti-rabbit IgG (1:200 dilution), rinsed in KPBS for 30 min and incubated for 1 h at RT with the avidin-biotin-peroxidase solution (1:100 dilution). After a 30-min rinse in 0.075 M PBS (pH 7.3), all sections were incubated for 15 min in 0.06% 3,3´-diaminobenzidine-HCl and 0.006% H_2O_2 diluted in PBS. Sections were rinsed, mounted on gelatin-coated slides, dehydrated and coverslipped with Permount (Fisher, Pittsburgh, Pennsylvania).

Some sections from control and pilocarpine-treated animals were double labeled to assess all neurons and somatostatin interneurons. Sections were incubated for 48 h at 4°C in somatostatin antiserum (1:4000) mixed with Neu-N monoclonal antibody (1:4000) in KPBS containing 0.5% milk protein (Boehringer Mannheim) and 0.3% Triton X-100. Then we detected somatostatin antiserum as described above, with a slight modification, including 0.03% of nickel ammonium sulphate in the incubation with DAB and H_2O_2 to obtain a dark blue product. We next detected the Neu-N antibody. We incubated sections for 1 h at RT in biotinylated horse anti-mouse IgG diluted 1:200 in KPBS containing 0.5% milk proteins, rinsed the sections in KPBS for 30 min, and incubated them for 1 h at RT with avidin-biotin-alkaline phosphatase solution (1:100). Visualization was done by incubating the sections with a fast red chromogen according to the manufacturer's recommendations, to obtain a red precipitate.

Somatostatin and calbindin were simultaneously detected in some sections from control and epileptic animals. Sections were incubated for 48 h at 4°C in somatostatin antiserum (1:2000) and calbindin monoclonal antibody (1:2000) diluted in KPBS containing 0.5% milk protein (Boehringer Mannheim) and 0.3% Triton X-100. After a 30-min rinse in KPBS, sections were incubated for 2 h at RT in biotinylated goat anti-rabbit IgG (1:200) and Cy3 goat anti-mouse IgG (1:100), rinsed in KPBS for 30 min, and incubated for 1 h at RT with avidin-FITC (1:100). Sections were rinsed, mounted on gelatin-coated slides, and coverslipped in an aqueous mounting medium (Gel/Mount, Biomeda, Foster City, California). Sections were examined with a Zeiss confocal microscope.

Quantitative studies of GAD mRNA- and somatostatin-containing neurons were done to determine the extent of cell loss in the stratum oriens of the CA1 region in pilocarpine-treated animals. For each population of cells, quantitative data were obtained from the stratum oriens in five sections each from control and pilocarpine-treated animals. In each section, the stratum oriens of the CA1 region was delineated, and the number of labeled neurons was plotted using a computer-assisted system (Neurolucida, Microbrightfield) with a Nikon microscope (Tokyo, Japan). Mean numbers of GAD mRNA- and somatostatin-containing neurons per 10,000 μm^2 were determined for each group of animals. For each cell population, the data were analyzed statistically by a mixed model analysis of variance (ANOVA) and Student's *t*-test.

Biocytin-filled neurons were detected on unsectioned slices. To neutralize endogenous peroxidase, slices were pretreated for 30 min in 1% H_2O_2. After several rinses in 0.1 M PBS (pH 7.4), slices were incubated for 24 h at RT, in 1:100 avidin-biotinylated peroxidase complex (Vector) diluted in PBS containing 0.3% Triton X-100. After 30 min rinses in PBS, slices were processed with 0.06% 3,3´-diaminobenzidine tetrahydrochloride (DAB, Sigma) and 0.006% H_2O_2 diluted in PBS. After histological processing, the general features of the recorded neurons were observed on a Nikon E800 microscope. A dent or a hole corresponding to the recording site was frequently observed in the membrane of the neurons. When observed for the dendritic recordings of pyramidal cells, its distance from the soma was calculated[23].

Electron microscopy. Hippocampal slices used for electrophysiological studies (from one control and one pilocarpine-treated rat) were prepared for electron microscopy as follows. Slices were transferred to 2% paraformaldehyde, 0.5% glutaraldehyde and 15% picric acid in 0.1 M phosphate buffer (pH 7.4) for 16 h at 4°C. Afterward, slices were cut at 50 µm on a vibratome and osmicated in 1% osmium tetroxide, dehydrated and embedded in Araldite resin. The embedded sections were trimmed and then re-sectioned serially into semi-thin (2 µm) sections with a Reichert Ultracut microtome. The sections were stained with 1% toluidine blue in 1% borax buffer. Neuropil from the stratum lacunosum-moleculare from CA1 regions was delimited light microscopically in the 2-µm sections. Selected semi-thin sections were then trimmed and resectioned at 60–70 nm for electron microscopy. Thin sections were collected on Formvar-coated, single-slot grids and were stained with uranyl acetate and lead citrate. The ultra-thin sections were examined with a Phillips-420 or a Jeol-1200 EX (Tokyo, Japan) electron microscope.

The sampling procedure consisted of 10 electron micrographs of neuropil from the stratum lacunosum moleculare and the stratum radiatum, taken at an initial magnification of 10,000× and printed at a final magnification of 30,000×. All synapses were identified following well-established morphological criteria[49], regardless of the angle of section at which the synaptic junctions were viewed (showing or not showing a synaptic cleft). Most synapses showing a synaptic cleft could be classified into asymmetrical (thick postsynaptic densities) or symmetrical (thin postsynaptic densities) synapses. Other synapses with no visible synaptic cleft or with postsynaptic densities that could not be clearly identified as symmetrical or asymmetrical were classified as uncharacterized.

The density of synapses (number/100 μm^2) was calculated. The relative numbers of synapses in stratum lacunosum moleculare and stratum radiatum between control and pilocarpine-treated animals were then estimated, taking into account the shrinkage, when observed, for these layers in epileptic rats. To calculate shrinkage, we measured the thickness of stratum lacunosum moleculare and stratum radiatum in slices prepared for electron microscopy, and in 50-µm vibratome sections stained with toluidine blue. The mean thickness of the stratum lacunosum moleculare measured on slices was 230 ± 14 µm and 133 ± 10 µm in control and pilocarpine-treated rats, respectively; a 42% shrinkage of this layer was observed in epileptic animals. The mean thickness of the stratum lacunosum moleculare assessed on sections was 144 ± 5 µm and 94 ± 5 µm in control and pilocarpine-treated rats, respectively; a 35% shrinkage of this layer was observed in epileptic animals. A mean shrinkage of 38% was used to estimate the number of synapses in stratum lacunosum moleculare of epileptic animals. The mean thickness of stratum radiatum was similar in control and pilocarpine-treated rats, when measured on slices (control, 476 ± 13 µm; pilocarpine, 458 ± 16 µm) or on sections (control, 274 ± 2 µm; pilocarpine, 265 ± 4 µm).

Data were analyzed by two-way analysis of variance (ANOVA) and Student's *t*-test. Counts and classification of synapses were made independently by two authors and then re-examined together.

ACKNOWLEDGEMENTS

We thank A.J. Tobin and N.J.K. Tillakaratne for the GAD67 cDNA and D. Diabira for the kainate-lesioned animals. This work was supported by I.N.S.E.R.M and the Simone and Cino del Duca Foundation.

RECEIVED 4 AUGUST; ACCEPTED 16 OCTOBER 2000

1. Prince, D. A. Neurophysiology of epilepsy. *Annu. Rev. Neurosci.* **1**, 395–415 (1978).
2. Obenaus, A., Esclapez, M. & Houser, C. R. Loss of glutamate decarboxylase mRNA-containing neurons in the rat dentate gyrus following pilocarpine-induced seizures. *J. Neurosci.* **13**, 4470–4485 (1993).
3. Sloviter, R. S. Decreased hippocampal inhibition and a selective loss of interneurons in experimental epilepsy. *Science* **235**, 73–76 (1987).
4. Houser, C. R. & Esclapez, M. Vulnerability and plasticity of the GABA system in the pilocarpine model of spontaneous recurrent seizures. *Epilepsy Res.* **26**, 207–218 (1996).
5. Morin, F., Beaulieu, C. & Lacaille, J. C. Selective loss of GABA neurons in area CA1 of the rat hippocampus after intraventricular kainate. *Epilepsy Res.* **32**, 363–369 (1998).
6. Mathern, G. W., Babb, T. L., Pretorius, J. K. & Leite, J. P. Reactive synaptogenesis and neuron densities for neuropeptide Y, somatostatin, and glutamate decarboxylase immunoreactivity in the epileptogenic human fascia dentata. *J. Neurosci* **15**, 3990–4004 (1995).

7. de Lanerolle, N. C., Kim, J. H., Robbins, R. J. & Spencer, D. D. Hippocampal interneuron loss and plasticity in human temporal lobe epilepsy. *Brain Res.* **495**, 387–395 (1989).
8. Robbins, R. J. *et al*. A selective loss of somatostatin in the hippocampus of patients with temporal lobe epilepsy. *Ann. Neurol.* **29**, 325–332 (1991).
9. Nusser, Z., Hajos, N., Somogyi, P. & Mody, I. Increased number of synaptic $GABA_A$ receptors underlies potentiation at hippocampal inhibitory synapses. *Nature* **395**, 172–177 (1998).
10. Gibbs, J. W., Shumate, M. D. & Coulter, D. A. Differential epilepsy-associated alterations in postsynaptic GABA(A) receptor function in dentate granule and CA1 neurons. *J. Neurophysiol.* **77**, 1924–1938 (1997).
11. Hirsch, J. C. *et al*. Deficit of quantal release of GABA in experimental models of temporal lobe epilepsy. *Nat. Neurosci.* **2**, 499–500 (1999).
12. Loup, F., Wieser, H. G., Yonekawa, Y., Aguzzi, A. & Fritschy, J. M. Selective alterations in $GABA_A$ receptor subtypes in human temporal lobe epilepsy. *J. Neurosci.* **20**, 5401–5419 (2000).
13. Buhl, E. H., Otis, T. S. & Mody, I. Zinc-induced collapse of augmented inhibition by GABA in a temporal lobe epilepsy model. *Science* **271**, 369–373 (1996).
14. Freund, T. F. & Buzsáki, G. Interneurons of the hippocampus. *Hippocampus* **6**, 347–470 (1996).
15. Miles, R., Tóth, K., Gulyás, A. I., Hájos, N. & Freund, T. F. Differences between somatic and dendritic inhibition in the hippocampus. *Neuron* **16**, 815–823 (1996).
16. Cohen, I. & Miles, R. Contributions of intrinsic and synaptic activities to the generation of neuronal discharges in in vitro hippocampus. *J. Physiol.(Lond.)*. **524**, 485–502 (2000).
17. Houser, C. R. & Esclapez, M. Localization of mRNAs encoding two forms of glutamic acid decarboxylase in the rat hippocampal formation. *Hippocampus* **4**, 530–545 (1994).
18. Katona, I., Acsady, L. & Freund, T. F. Postsynaptic targets of somatostatin-immunoreactive interneurons in the rat hippocampus. *Neuroscience* **88**, 37–55 (1999).
19. Tóth, K. & Freund, T. F. Calbindin D28k-containing nonpyramidal cells in the rat hippocampus: their immunoreactivity for GABA and projection to the medial septum. *Neuroscience* **49**, 793–805 (1992).
20. Fricker, D., Verheugen, J. A. & Miles, R. Cell-attached measurements of the firing threshold of rat hippocampal neurones. *J. Physiol.(Lond.)* **517**, 791–804 (1999).
21. Esclapez, M., Hirsch, J. C., Ben-Ari, Y. & Bernard, C. Newly formed excitatory pathways provide a substrate for hyperexcitability in experimental temporal lobe epilepsy. *J. Comp. Neurol.* **408**, 449–460 (1999).
22. Lacaille, J.-C. & Williams, S. Membrane properties of interneurons in stratum oriens-alveus of the CA1 region of rat hippocampus in vitro. *Neuroscience* **36**, 349–359 (1990).
23. Cossart, R. *et al*. Distribution of spontaneous currents along the somato-dendritic axis of rat hippocampal CA1 pyramidal neurons. *Neuroscience* **99**, 593–603 (2000).
24. Yanovsky, Y., Sergeeva, O. A., Freund, T. F. & Haas, H. L. Activation of interneurons at the stratum oriens/alveus border suppresses excitatory transmission to apical dendrites in the CA1 area of the mouse hippocampus. *Neuroscience* **77**, 87–96 (1997).
25. Hirsch, J. C. *et al*. Enhanced NMDAR-dependent epileptiform activity is controlled by oxidizing agents in a chronic model of temporal lobe epilepsy. *J. Neurophysiol.* **76**, 4185–4189 (1996).
26. Maccaferri, G. & McBain, C. J. Passive propagation of LTD to stratum oriens–alveus inhibitory neurons modulates the temporoammonic input to the hippocampal CA1 region. *Neuron* **15**, 137–145 (1995).
27. Buckmaster, P. S. & Jongen-Relo, A. L. Highly specific neuron loss preserves lateral inhibitory circuits in the dentate gyrus of kainate-induced epileptic rats. *J. Neurosci.* **19**, 9519–9529 (1999).
28. Maccaferri, G., Roberts, J. D., Szucs, P., Cottingham, C. A. & Somogyi, P. Cell surface domain specific postsynaptic currents evoked by identified GABAergic neurones in rat hippocampus in vitro. *J. Physiol.(Lond.)* **524**, 91–116 (2000).
29. Oliva, A. A. J., Jiang, M., Lam, T., Smith, K. L. & Swann, J. W. Novel hippocampal interneuronal subtypes identified using transgenic mice that express green fluorescent protein in GABAergic interneurons. *J. Neurosci.* **20**, 3354–3368 (2000).
30. Liu, Z., Nagao, T., Desjardins, G. C., Gloor, P. & Avoli, M. Quantitative evaluation of neuronal loss in the dorsal hippocampus in rats with long-term pilocarpine seizures. *Epilepsy Res.* **17**, 237–247 (1994).
31. Pyapali, G. K. & Turner, D. A. Denervation-induced dendritic alterations in CA1 pyramidal cells following kainic acid hippocampal lesions in rats. *Brain Res.* **652**, 279–290 (1994).
32. Houser, C. R. Neuronal loss and synaptic reorganization in temporal lobe epilepsy. *Adv. Neurol.* **79**, 743–761 (1999).
33. Perez, Y., Morin, F., Beaulieu, C. & Lacaille, J.-C. Axonal sprouting of CA1 pyramidal cells in hyperexcitable hippocampal slices of kainate-treated rats. *Eur. J. Neurosci.* **8**, 736–748 (1996).
34. Ross, S. T. & Soltesz, I. Selective depolarization of interneurons in the early posttraumatic dentate gyrus: involvement of the Na^+/K^+-ATPase. *J. Neurophysiol.* **83**, 2916–2930 (2000).
35. Rempe, D. A., Bertram, E. H., Williamson, J. M. & Lothman, E. W. Interneurons in area CA1 stratum radiatum and stratum oriens remain functionally connected to excitatory synaptic input in chronically epileptic animals. *J. Neurophysiol.* **78**, 1504–1515 (1997).
36. Esclapez, M., Hirsch, J. C., Khazipov, R., Ben-Ari, Y. & Bernard, C. Operative GABAergic inhibition in hippocampal CA1 pyramidal neurons in experimental epilepsy. *Proc. Natl. Acad. Sci. USA* **94**, 12151–12156 (1997).
37. Chen, K., Baram, T. Z. & Soltesz, I. Febrile seizures in the developing brain result in persistent modifications of neuronal excitability in limbic circuits. *Nat. Med.* **5**, 888–894 (1999).
38. Prince, D. A. & Jacobs, K. Inhibitory function in two models of chronic epileptogenesis. *Epilepsy Res.* **32**, 83–92 (1998).
39. Otis, T. S., De Koninck, Y. & Mody, I. Lasting potentiation of inhibition is associated with an increased number of gamma-aminobutyric acid type A receptors activated during miniature inhibitory postsynaptic currents. *Proc. Natl. Acad. Sci. USA*. **91**, 7698–7702 (1994).
40. Magee, J. C. & Cook, E. P. Somatic EPSP amplitude is independent of synapse location in hippocampal pyramidal neurons. *Nat. Neurosci.* **3**, 895–903 (2000).
41. Holmes, W. R. & Levy, W. B. Quantifying the role of inhibition in associative long-term potentiation in dentate granule cells with computational models. *J. Neurophysiol.* **78**, 103–116 (1997).
42. Kapur, A., Lytton, W. W., Ketchum, K. L. & Haberly, L. B. Regulation of the NMDA component of EPSPs by different components of postsynaptic GABAergic inhibition: Computer simulation analysis in piriform cortex. *J. Neurophysiol.* **78**, 2546–2559 (1997).
43. Johnston, D., Hoffman, D. A., Colbert, C. M. & Magee, J. C. Regulation of back-propagating action potentials in hippocampal neurons. *Curr. Opin. Neurobiol.* **9**, 288–292 (1999).
44. Nadler, J. V. Kainic acid as a tool for the study of temporal lobe epilepsy. *Life Sci.* **29**, 2031–2042 (1981).
45. Kaufman, D. L., McGinnis, J. F., Krieger, N. R. & Tobin, A. J. Brain glutamate decarboxylase cloned in lambda gt-11: fusion protein produces gamma-aminobutyric acid. *Science* **232**, 1138–1140 (1986).
46. Goodman, R. H., Jacobs, J. W., Dee, P. C. & Habener, J. F. Somatostatin-28 encoded in a cloned cDNA obtained from a rat medullary thyroid carcinoma. *J. Biol. Chem.* **257**, 1156–1159 (1982).
47. Esclapez, M., Tillakaratne, N. J. K., Kaufman, D. L., Tobin, A. J. & Houser, C. R. Comparative localization of two forms of glutamic acid decarboxylase and their mRNAs in rat brain supports the concept of functional differences between the forms. *J. Neurosci.* **14**, 1834–1855 (1994).
48. Kaufman, D. L., Houser, C. R. & Tobin, A. J. Two forms of the gamma-aminobutyric acid synthetic enzyme glutamate decarboxylase have distinct intraneuronal distributions and cofactor interactions. *J. Neurochem.* **56**, 720–723 (1991).
49. Peters, A. & Palay, S. L. The morphology of synapses. *J. Neurocytol.* **25**, 687–700 (1996).